



Topology Optimization fiber reinforced materials considering Tsai-Wu yield criterion

Andre Luis Ferreira da Silva¹, Eduardo Moscatelli¹, Emilio Carlos Nelli Silva¹

¹*Dept. of Mechatronics and Mechanical Systems Engineering, University of São Paulo
Av. Prof. Mello Moraes, 2231, 05508-030, São Paulo/SP, Brazil
andre.fersi@usp.br*

Abstract. The utilization of fiber-reinforced materials has experienced a significant surge due to their notable advantages, particularly their high strength-to-mass ratio. As a result, new additive manufacturing technologies have emerged to accommodate these materials, offering capabilities for tailoring fiber orientation and creating opportunities for optimization techniques. Consequently, a growing body of literature has focused on optimizing fiber orientation. However, a crucial consideration in this context is the stress yield criteria. This study addresses the Topology Optimization problem by minimizing the structure volume while considering local stress constraints using Tsai-Wu yield criteria. To achieve this, we use the method NDFO-adapt, which determines the material distribution and fiber orientation. Our approach optimizes the penalization fields, material distribution, and fiber angles. Additionally, we extend a similar approach to optimize the threshold projection parameter. By adopting this strategy, we modify the solution space, enabling the exploration of previously unattainable local minima. To handle the local stress constraint, we employ the Augmented Lagrangian method. The efficacy of the proposed method is demonstrated through numerical examples.

Keywords: Topology Optimization, Fiber-reinforced materials, Local stress constraints, Tsai-Wu, Multiple design variables

1 Introduction

The increasing use of fiber-reinforced materials, known for their high strength-to-mass ratio, has led to the development of additive manufacturing techniques (Palanikumar et al. [1], Ning et al. [2], Quan et al. [3], Hou et al. [4], Dickson et al. [5]). For this reason, plenty of works are being developed in the literature to solve the problem of optimizing the fiber orientation in this material. Some works employ heuristic algorithms for optimizing fiber orientation, offering potential "global minima" solutions without extensive gradient calculations. Examples include Kim et al. [6] and António [7]. However, the efficiency of non-gradient methods for complex multi-variable problems is debated Sigmund [8]. Another avenue involves the homogenization method Allaire et al. [9], building on Pedersen [10] work on minimizing compliance through principal strain tensor directions. Gradient-based techniques, seen in works like Soares et al. [11] and Luo and Gea [12], treat angles as direct design variables, leading to challenges of local minima and sensitivity to initial assumptions. Stegmann and Lund [13] introduced an interpolation material model, later extended by Bruyneel [14] and Gao et al. [15]. Challenges arise with an increase in candidates leading to more design variables. Kiyono et al. [16] addressed this with normal distribution functions, while Salas et al. [17] used Taylor series approximations. Salas et al. [18] hybridized these techniques. Stress constraints are often overlooked despite these advancements, even in isotropic cases. This study introduces NDFO-adapt, optimizing both fiber orientation and material distribution in fiber-reinforced structures using the well-established interpolation material model SIMP [19]. The innovative aspect lies in an adaptive penalization field optimized alongside material distribution and fiber angle parameters, addressing the balance between fiber optimization and stress constraints considering Tsai-Wu yield criteria.

2 Theoretical formulation

This work considers the hypothesis of small displacements, strain, and rotation: linear elastic setting. The field equation of solid mechanics represents the forward problem associated with the Topology Optimization problem in its weak form (Zienkiewicz and Taylor [20], Bendsoe and Sigmund [21]):

$$a(\mathbf{u}, \mathbf{v}) = L(\mathbf{v}) \quad (1)$$

where the *Energy bilinear form* and *Load linear form* are defined as:

$$a(\mathbf{u}, \mathbf{v}) = \int_{\Omega} \sigma_{ij}(\mathbf{u}) \epsilon_{ij}(\mathbf{v}) d\Omega \quad (2)$$

The i^{th} components of the body force and the surface force are defined by b_i and t_i , while v_i is the i^{th} component of the virtual displacement vector. The components ij of the Cauchy stress tensor and the linear strain tensor, σ_{ij} and ϵ_{ij} , respectively, are calculated as:

$$\sigma_{ij} = C_{ijkl} \epsilon_{jk}(\mathbf{u}) \quad (3)$$

$$\epsilon_{ij} = \frac{1}{2} \left(\frac{\partial u_i}{\partial x_j} + \frac{\partial u_j}{\partial x_i} \right) \quad (4)$$

The C_{ijkl} represents the $ijkl$ component of the constitutive tensor \mathbf{C} , which is calculated by using the constitutive tensor for an orthotropic material \mathbf{Q} , the Reuter matrix \mathbf{R} and the transformation tensor \mathbf{T} , as defined by Kaw [22]:

$$\mathbf{C} = \mathbf{T}^{-1} \mathbf{Q} \mathbf{R} \mathbf{T} \mathbf{R}^{-1} \quad (5)$$

The interpolation material model is the well-known SIMP Bendsoe [19], where a pseudo-density variable multiplies the constitutive tensor, that is:

$$\sigma_{ij} = (\rho_{min} + (1 - \rho_{min}) \tilde{\rho}^p) C_{ijkl} \epsilon_{kl}(\mathbf{u}) \quad (6)$$

where ρ_{min} is a minimal value for the pseudo-density ρ , which varies from 0 to 1, $\tilde{\rho}$ is the physical pseudo-densities field and \tilde{p} is the filtered penalization for SIMP material model. The penalization p is also considered a design variable optimized with the pseudo-densities.

The optimized fiber angle orientation is calculated using the interpolation material model NDFO-adap (da Silva et al. [23]). The penalization parameter of the NDFO-adap, named p_n , is optimized together with the other design variable. The physical fiber angle $\tilde{\phi}$ is defined by using the weighted sum:

$$\tilde{\phi} = \sum_{i=1}^{N_c} w_i \phi_i^c \quad (7)$$

where N_c is the number candidate angles, ϕ^c are the candidate angles, and w is the weight function that defined as:

$$w_i = \frac{\hat{w}_i}{\sum_{j=1}^{N_c} \hat{w}_j} \quad (8)$$

The normal distribution function \hat{w} is defined by:

$$\hat{w}_i = \exp \left(-\frac{(\tilde{\phi} - \phi_i^c)^2}{2 \tilde{p}_n^2} \right) \quad (9)$$

where $\tilde{\phi}$ represents the field of filtered fiber angles, and \tilde{p}_n is the filtered field of penalization for the NDFO-adap interpolation material model.

To help the pseudo-densities reach the values of 0 and 1, which represent void and material in the domain, we use the threshold projection proposed by Xu et al. [24] in the *tanh* form:

$$\tilde{\rho} = \frac{\tanh(\tilde{\beta} \eta + \tanh(\tilde{\beta}(\tilde{\rho} - \eta)))}{\tanh(\tilde{\beta} \eta) + \tanh(\tilde{\beta}(1 - \eta))} \quad (10)$$

where $\tilde{\beta}$ is the filtered projection field and η is an inflection parameter.

The Topology Optimization problem has as its objective to minimize the structure volume considering compliance and stress constraints:

$$\begin{aligned} \min_{\rho, \phi, p, p_n, \beta} \quad & J = \frac{\int_{\Omega} \tilde{\rho} d\Omega}{V} \\ \text{such that} \quad & F = a(\mathbf{u}, \mathbf{v}, \tilde{\rho}, \tilde{\phi}) - L(\mathbf{v}) = 0 \\ & G_1^{(e)} = f_{\sigma}^{(e)} \sigma_{tw}^{(e)} \left(\left(f_{\sigma}^{(e)} \sigma_{tw}^{(e)} \right)^2 + 1 \right) \leq 0 \\ & G_2 = \left(\frac{c(\mathbf{u}, \tilde{\rho}, \tilde{\phi})}{\alpha_c c_{full}(\mathbf{u}, \phi_{princ})} - 1 \right) \left(\left(\frac{c(\mathbf{u}, \tilde{\rho}, \tilde{\phi})}{\alpha_c c_{full}(\mathbf{u}, \phi_{princ})} - 1 \right)^2 + 1 \right) \leq 0 \\ & \rho_{min} \leq \rho_{lb}(g, g_{gl}) \leq \rho \leq \rho_{ub}(g, g_{gl}) \leq 1 \\ & \phi_{min} \leq \phi \leq \phi_{max} \\ & p_{min}(g) \leq p \leq p_{max} \\ & p_{n_{min}} \leq p_{n_{lb}} \leq p_n \leq p_{n_{max}} \\ & \beta_{min}(g) \leq \beta \leq \beta_{max} \end{aligned} \quad (11)$$

where J represents the volume fraction of the structure, F is the state equation, $G_1^{(e)}$ is the local stress constraint, G_2 is the compliance constraint, and all others are box constraints.

The term σ_{tw} represents the left-hand side of the Tsai-Wu yield criterion:

$$H_1 \sigma_1 + H_2 \sigma_2 + H_6 \sigma_6 + H_{11} \sigma_1^2 + H_{22} \sigma_2^2 + H_{66} \sigma_6^2 + 2 H_{12} \sigma_1 \sigma_2 - 1 < 0 \quad (12)$$

where σ_i , $i = 1, 2, 6$, are components of the Cauchy stress tensor in the fiber directions, and the H terms are calculated as a function of the ultimate longitudinal tensile strength $(\sigma_1^T)_{ult}$, the ultimate longitudinal compressive strength $(\sigma_1^C)_{ult}$, the ultimate transverse tensile strength $(\sigma_2^T)_{ult}$, the ultimate transverse compressive strength $(\sigma_2^C)_{ult}$, and the ultimate in-plane shear strength, according to [22]:

$$H_{\alpha} = \frac{1}{(\sigma_{\alpha}^T)_{ult}} - \frac{1}{(\sigma_{\alpha}^C)_{ult}} \quad \alpha = 1, 2 \quad (13a)$$

$$H_{\alpha\alpha} = \frac{1}{(\sigma_{\alpha}^T)_{ult} (\sigma_{\alpha}^C)_{ult}} \quad \alpha = 1, 2 \quad (13b)$$

$$H_6 = 0 \quad (13c)$$

$$H_{66} = \frac{1}{(\sigma_6)_{ult}^2} \quad (13d)$$

$$H_{12} = -\frac{1}{2} \sqrt{\frac{1}{(\sigma_1^T)_{ult} (\sigma_1^C)_{ult} (\sigma_2^T)_{ult} (\sigma_2^C)_{ult}}} \quad (13e)$$

The compliance constraint is a comparison between the compliance of the optimized structure in the current iteration c with the compliance full c_{full} , which is the compliance calculated considering that the pseudo-density ρ is equal to one in the whole structure and that the fiber orientation is equal to principal stress direction:

$$c = \int_{\Omega} \sigma_{ij}(\mathbf{u}, \tilde{\rho}, \tilde{\phi}) \frac{\partial u_i}{\partial x_j} d\Omega \quad (14)$$

$$c_{full}(\mathbf{u}, \phi_{princ}) = \int_{\Omega} \sigma_{ij}(\mathbf{u}, \phi_{princ}) \frac{\partial u_i}{\partial x_j} d\Omega \quad (15)$$

The problem is implemented using the Augmented Lagrangian method in FEniCS project software. The sensitivities are calculated using an automatic differentiation software named Dolfin-Adjoint, and the optimization is performed using an L-BFGS-B algorithm implemented in the SciPy library. The optimization flowchart is presented in the Fig. 1

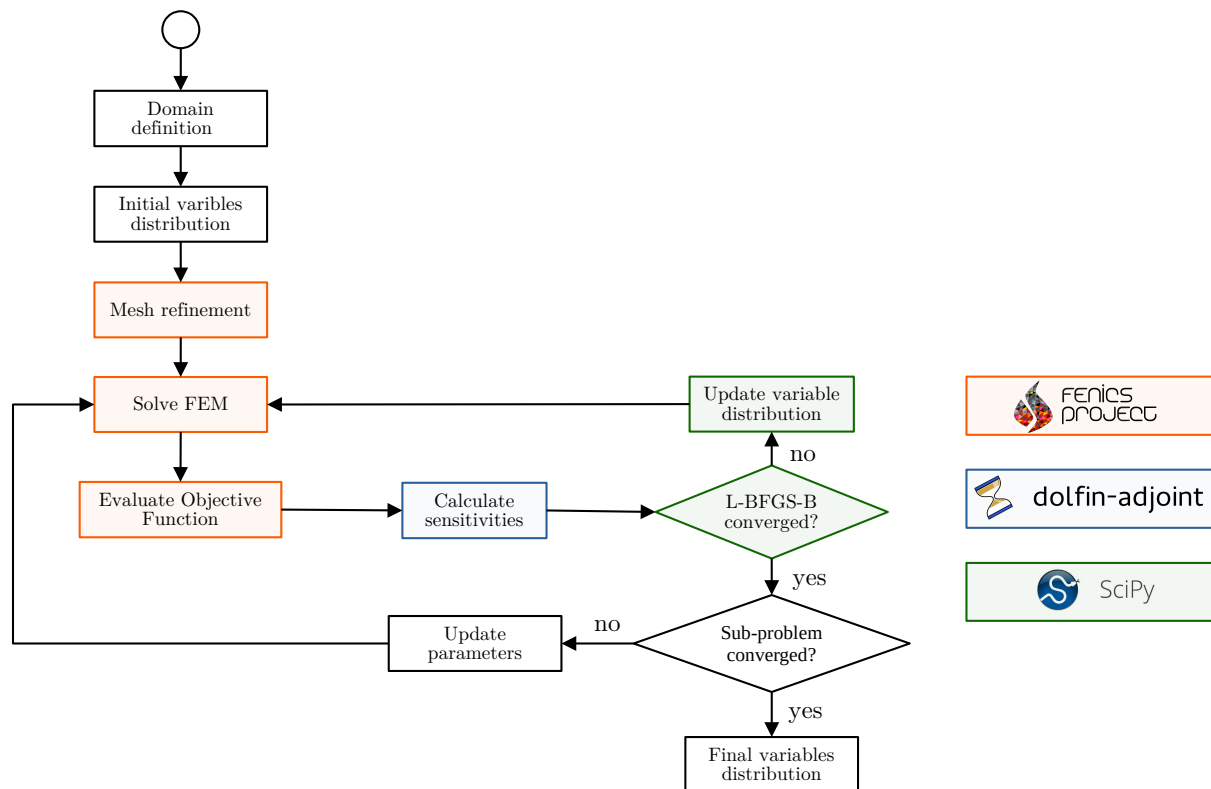


Figure 1. Topology optimization flowchart

3 Results

Two results for the L-bracket represented by Fig. 2 are presented. The material considered in the simulations is graphite/epoxy. The material properties for a composite with a fiber volume fraction of 0.45 are shown in the in section 3 [22].

Results obtained using two different values of α_c , the variable used in the compliance constraint, are presented in Fig. 3. Fig. 3a and Fig. 3b show the optimized fiber orientation for $\alpha_c = 4$ and $\alpha_c = 5$, respectively. The objective function J for the case where α_c is equal to 4 is approximately 0.41, while for the case where α_c is 5, the objective function is equal to 0.39. It is expected that the volume fraction will be smaller for smaller compliance as well, considering that more material increases the structure's stiffness. For both cases, it is possible to observe stress relief in the corner of the structure, as highlighted in Detail 1. Also, for both results, we observe that the fibers follow the path created by the material distribution, ensuring fiber continuity. Fiber discontinuities can be observed

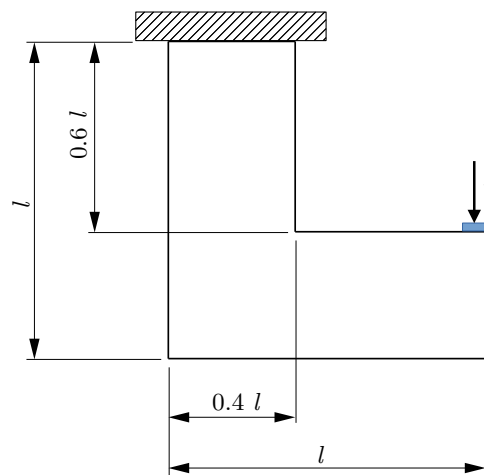


Figure 2. L-bracket domain

E_1	E_2	G_{12}	ν_{12}	$(\sigma_1^T)_{ult}$	(σ_1^C)	$(\sigma_2^T)_{ult}$	$(\sigma_2^C)_{ult}$	$(\sigma_6)_{ult}$
181 GPa	10.3 GPa	7.17 GPa	0.28	1500 MPa	1500 MPa	40 MPa	246 MPa	72 MPa

in regions with two or more members, as shown in Details 2 and 3. As can be observed in Figs. 3c and 3d, the maximum values of stress constraints are in an order of $1 \cdot 10^{-2}$, that is, very close to zero.

4 Conclusions

In this study, we successfully implemented a topology optimization algorithm that effectively optimized fields of fiber orientation, material distribution, and penalizations, considering the Tsai-Wu yield criterion for stress constraint and a compliance constraint. The final fiber distribution tends to follow the path formed by the material distribution, with exceptions in places with two or more members. Both examples present stress relief in the corner of the structure. The stress constraint is respected in the structure, but some feel elements where its value is in order of $1 \cdot 10^{-2}$, very close to 0.

Acknowledgements. We gratefully acknowledge the support of the RCGI - Research Centre for Gas Innovation, hosted by the University of São Paulo (USP) and sponsored by FAPESP - São Paulo Research Foundation (2014/50279-4) and Shell Brasil, and the strategic importance of the support given by ANP (Brazil's National Oil, Natural Gas and Biofuels Agency) through the RD levy regulation. Moreover, the first author (A.L.F. Silva) thanks FAPESP (São Paulo Research Foundation) for their doctoral fellowships with numbers 2020/07557-4. Besides, the first author (A.L.F. Silva) thanks INCT/CEMTEC (National Institute on Advanced Eco-Efficient Cement-Based Technologies). The third author (E.C.N. Silva) is pleased to acknowledge CNPq's (National Council for Scientific and Technological Development) support under grant 302658/2018-1.

Authorship statement. The authors hereby confirm that they are the sole liable persons responsible for the authorship of this work, and that all material that has been herein included as part of the present paper is either the property (and authorship) of the authors, or has the permission of the owners to be included here.

References

- [1] K. Palanikumar, M. Mudhukrishnan, and P. Soorya Prabha. Technologies in additive manufacturing for fiber reinforced composite materials: a review. *Current Opinion in Chemical Engineering*, vol. 28, pp. 51–59, 2020.
- [2] F. Ning, W. Cong, J. Qiu, J. Wei, and S. Wang. Additive manufacturing of carbon fiber reinforced thermoplastic composites using fused deposition modeling. *Composites Part B: Engineering*, vol. 80, pp. 369–378, 2015.
- [3] Z. Quan, A. Wu, M. Keefe, X. Qin, J. Yu, J. Suhr, J.-H. Byun, B.-S. Kim, and T.-W. Chou. Additive manufacturing of multi-directional preforms for composites: opportunities and challenges. *Materials Today*, vol. 18, n. 9, pp. 503–512, 2015.
- [4] Z. Hou, X. Tian, J. Zhang, and D. Li. 3d printed continuous fibre reinforced composite corrugated structure. *Composite Structures*, vol. 184, pp. 1005–1010, 2018.
- [5] A. N. Dickson, K.-A. Ross, and D. P. Dowling. Additive manufacturing of woven carbon fibre polymer composites. *Composite Structures*, vol. 206, pp. 637–643, 2018.
- [6] J.-S. Kim, C.-G. Kim, and C.-S. Hong. Optimum design of composite structures with ply drop using genetic algorithm and expert system shell. *Composite Structures*, vol. 46, n. 2, pp. 171–187, 1999.
- [7] C. A. C. António. A hierarchical genetic algorithm with age structure for multimodal optimal design of hybrid composites. *Structural and Multidisciplinary Optimization*, vol. 31, n. 4, pp. 280–294, 2006.
- [8] O. Sigmund. On the usefulness of non-gradient approaches in topology optimization. *Structural and Multidisciplinary Optimization*, vol. 43, n. 5, pp. 589–596, 2011.
- [9] G. Allaire, P. Geoffroy-Donders, and O. Pantz. Topology optimization of modulated and oriented periodic microstructures by the homogenization method. *Computers & Mathematics with Applications*, vol. 78, n. 7, pp. 2197–2229, 2019.
- [10] P. Pedersen. On optimal orientation of orthotropic materials. *Structural Optimization*, vol. 1, n. 2, pp. 101–106, 1989.
- [11] C. Soares, C. Soares, and H. Mateus. A model for the optimum design of thin laminated plate-shell structures for static, dynamic and buckling behaviour. *Composite Structures*, vol. 32, n. 1-4, pp. 69–79, 1995.

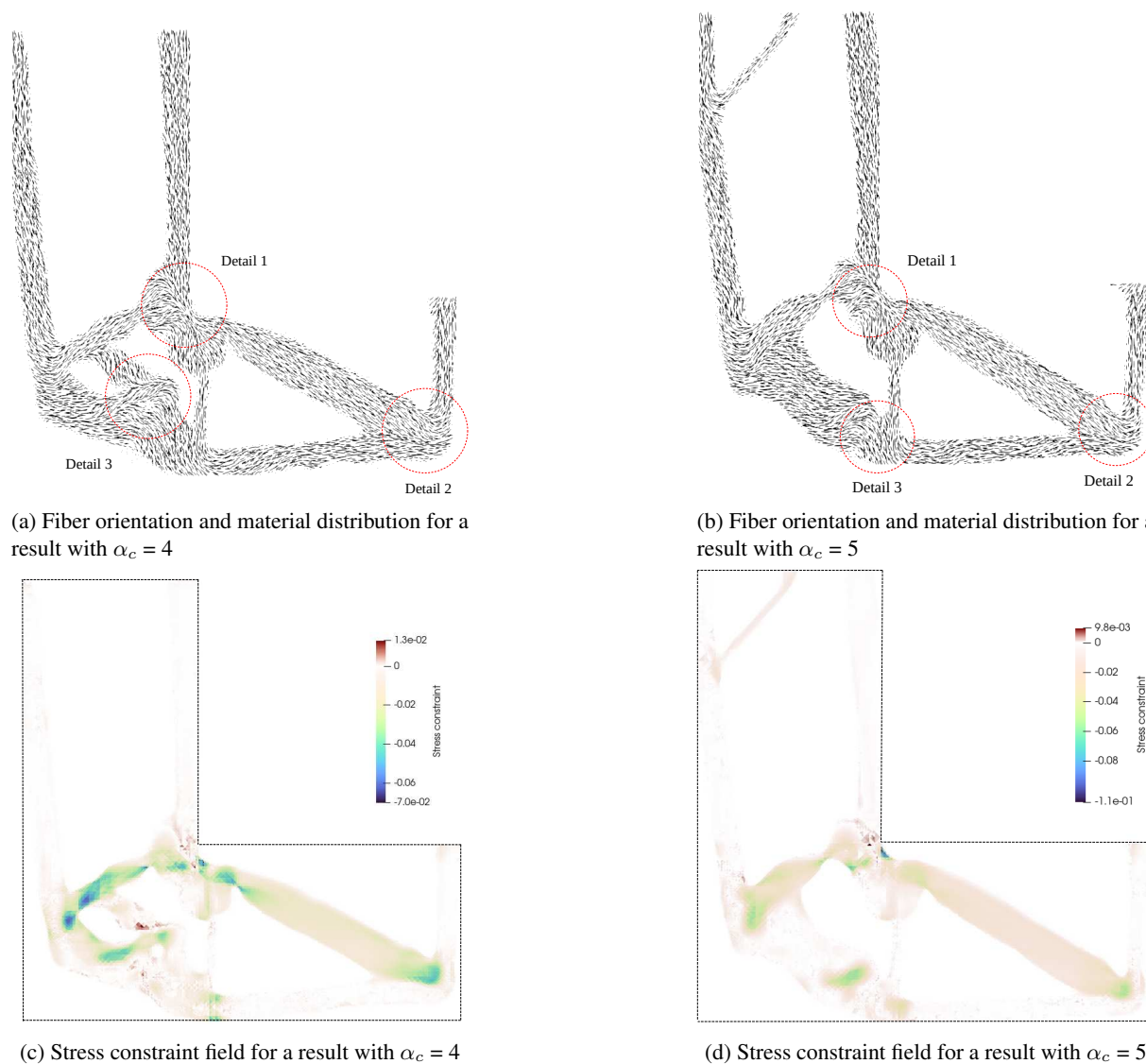


Figure 3. Fibers and stress constraints fields for two different values of α_c

- [12] J. H. Luo and H. C. Gea. Optimal bead orientation of 3d shell/plate structures. *Finite Elements in Analysis and Design*, vol. 31, n. 1, pp. 55–71, 1998.
- [13] J. Stegmann and E. Lund. Discrete material optimization of general composite shell structures. *Int J Numer Meth Eng*, vol. 62, n. 14, pp. 2009–2027, 2005.
- [14] M. Bruyneel. SFP—a new parameterization based on shape functions for optimal material selection: application to conventional composite plies. *Structural and Multidisciplinary Optimization*, vol. 43, n. 1, pp. 17–27, 2010.
- [15] T. Gao, W. Zhang, and P. Duysinx. A bi-value coding parameterization scheme for the discrete optimal orientation design of the composite laminate. *International Journal for Numerical Methods in Engineering*, vol. 91, n. 1, pp. 98–114, 2012.
- [16] C. Y. Kiyono, E. C. N. Silva, and J. N. Reddy. A novel fiber optimization method based on normal distribution function with continuously varying fiber path. *Compos Struct*, vol. 160, pp. 503–515, 2017.
- [17] R. A. Salas, F. J. Ramírez-Gil, W. Montealegre-Rubio, E. C. N. Silva, and J. Reddy. Optimized dynamic design of laminated piezocomposite multi-entry actuators considering fiber orientation. *Computer Methods in Applied Mechanics and Engineering*, vol. 335, pp. 223–254, 2018.
- [18] R. A. Salas, da A. L. F. Silva, and E. C. N. Silva. HYIMFO: Hybrid method for optimizing fiber orientation angles in laminated piezocomposite actuators. *Comput Method Appl M*, vol. 385, pp. 114010, 2021.
- [19] M. P. Bendsøe. Optimal shape design as a material distribution problem. *Structural Optimization*, vol. 1, n. 4, pp. 193–202, 1989.
- [20] O. C. Zienkiewicz and R. L. Taylor. *The finite element method for solid and structural mechanics*. Elsevier, 2005.
- [21] M. P. Bendsoe and O. Sigmund. *Topology optimization: theory, methods, and applications*. Springer Science & Business Media, 2003.
- [22] A. K. Kaw. *Mechanics of composite materials*. CRC press, 2005.
- [23] da A. L. F. Silva, R. A. Salas, and E. C. N. Silva. Topology optimization of fiber reinforced structures considering stress constraint and optimized penalization. *Composite Structures*, vol. 316, pp. 117006, 2023.
- [24] S. Xu, Y. Cai, and G. Cheng. Volume preserving nonlinear density filter based on heaviside functions. *Struct Multidiscip O*, vol. 41, n. 4, pp. 495–505, 2009.